Supporting Information for

Modulated Synthesis and Isoreticular Expansion of Th-MOFs with Record High Pore Volume and Surface Area for Iodine Adsorption

Zi-Jian Li,[a] Yu Ju,[a,b] Bowen Yu,[a] Xiaoling Wu,[a] Huangjie Lu,[a] Yongxin Li,[c] Jing Zhou,[a] Xiaofeng Guo,[d] Zhi-Hui Zhang,[b] Jian Lin,[a] Jian-Qiang Wang, [a,e] and Shuao Wangf*[a]

Key Laboratory of Interfacial Physics and Technology, Shanghai Institute of Applied Physics, Chinese Academy of Sciences, 2019 Jia Luo Road, Shanghai 201800, China.

[b] Jiangsu Key Laboratory of Advanced Catalytic Materials and Technology, Changzhou University, Changzhou 213164, China

[c] Division of Chemistry and Biological Chemistry, School of Physical and Mathematical Sciences, Nanyang Technological University, 637371, Singapore

[d] Department of Chemistry and Alexandra Navrotsky Institute for Experimental Thermodynamics, Washington State University, Pullman, WA 99164-4630, USA

[e] Dalian National Laboratory for Clean Energy, Dalian 116023, China

[f] Radiologicaland Interdisciplinary Sciences (RAD-X) and Collaborative Innovation Centre of Radiological Medicine of Jiangsu Higher Education Institutions, Soochow University,Suzhou 215123, China.

Table of Content

S1. EXPERIMENTAL SECTION

S1.1 Synthesis

Materials and Synthesis. $Th(NO_3)_4·6H_2O$ (99%, Changchun Institute of Applied Chemistry, Chinese Academy of Sciences), formic acid (HCOOH, 98%+, Adamas), concentrated HCl (36.0~38.0%, Sinopharm Chemical Reagent Co.,Ltd), concentrated HNO_3 (65.0～68.0%, Sinopharm Chemical Reagent Co.,Ltd), CF_3COOH (99%, Adamas), terephthalic acid (99%, Adamas), biphenyldicarboxylic acid (99%, Adamas), fumaric acid (99%, Adamas), 4-carboxycinnamic acid (99%, Adamas), 1,4-phenylenediacrylic acid (99%, Adamas), 4,4-azobenezenedicarboxylic acid (98%, Jilin Chinese Academy of Sciences - Yanshen Technology Co., Ltd), 4,4'-stilbenedicarboxylic acid (99%, Adamas), *N,N'*-Dimethylformamide (DMF, 99%, Adamas), dichloromethane (DCM, 99.5%, Greagent), tetrahydrofuran (THF, 99.5%, Adamas), acetonitrile (CH_3CN, ≥ 99.0%, Greagent), acetone (99.5%, Sinopharm Chemical Reagent Co.,Ltd), n-hexane (97%, SafeDry, Adamas), diethyl ether (99%, Sinopharm Chemical Reagent Co.,Ltd), cyclohexane (99%+, Adamas), and iodine (I_2, 99%, Adamas) were used as received and without further purification.

Caution! ^{232}Th used in this study is an α emitter with the daughter of radioactive Ra-228. All thorium compounds used and investigated were operated in an authorized laboratory designed for actinide element studies. Standard precautions for handling radioactive materials should be followed.

Th-SINAP-9. A mixture of $Th(NO_3)_4·6H_2O$ (4.7 mg, 0.008 mmol), fumaric acid (H_2FUM, 0.46 mg, 0.004 mmol), DMF (0.37 mL), HCOOH (0.04 mL) in a capped vial was heated at 120 °C for 24 h. Colourless octahedral crystals were filtered, washed with MeOH and Et_2O, and dried at room temperature. The pH values before and after reaction are 2.07 and 5.09, respectively. Yield, 36% based on H_2FUM. Anal. Calcd for $Th_6(\mu_3\text{-}O)_4(\mu_3\text{-}OH)_4(FUM)_6(H_2O)_6(C_3H_7NO)_{11}(H_2O)_{19}$, $C_{57}H_{143}N_{11}Th_6O_{68}$, C, 19.77; H, 4.16; N, 4.45. Found: C, 19.78; H, 4.39; N, 4.53%. IR: 1655 (s), 1574(s), 1386 (vs), 1201 (w), 1103 (w), 798 (w), 666 (m), 600 (m), 529 (s) cm^{-1}. Microcrystalline powder can be obtained as followed: A mixture of $Th(NO_3)_4·6H_2O$ (23.5 mg, 0.04 mmol), fumaric acid (2.3 mg, 0.02 mmol), DMF (0.69 mL), HCOOH (0.02 mL), H_2O (0.15 mL) in a capped vial was heated at 120 °C for 24 h. Colourless microcrystals were filtered, washed with MeOH and Et_2O, and dried at room temperature.

Th-SINAP-10. A mixture of $Th(NO_3)_4·6H_2O$ (4.7 mg, 0.008 mmol), terephthalic acid (H_2BDC, 0.66 mg, 0.004 mmol), DMF (0.38 mL), HCOOH (0.045 mL) or concentrated HNO_3 (0.035 mL) or CF_3COOH (0.03 mL) in a capped vial was heated at 120 °C for 24 h. Colourless octahedral crystals were filtered, washed with MeOH and Et_2O, and dried at room temperature. The pH values before and after reaction for HCOOH, CF_3COOH, and conc. HNO_3 are 2.12/5.04, 1.34/5.52, and 0.63/5.09, respectively. Yield, 36% based on H_2BDC. Anal. Calcd for $Th_6(\mu_3\text{-}O)_4(\mu_3\text{-}OH)_4(BDC)_{12}(H_2O)_6(C_3H_7NO)_{11}(H_2O)_9$, $C_{81}H_{135}N_{11}Th_6O_{58}$, C, 27.15; H, 3.80; N, 4.30. Found: C, 27.46; H, 3.69; N, 4.23%. IR: 1651 (s), 1583 (vs), 1502 (m), 1382 (vs), 1201 (w), 1096 (w), 747 (m), 506 (m) cm^{-1}. Microcrystalline powder can be obtained

as followed: A mixture of $Th(NO_3)_4 \cdot 6H_2O$ (23.5 mg, 0.04 mmol), terephthalic acid (3.3 mg, 0.02 mmol), DMF (0.69 mL), CF_3COOH (0.06 mL), H_2O (0.06 mL)in a capped vial was heated at 120 °C for 48 h. Colourless microcrystals were filtered, washed with MeOH and Et_2O, and dried at room temperature.

Th-SINAP-11. A mixture of $Th(NO_3)_4 \cdot 6H_2O$ (4.7 mg, 0.008 mmol), 4-carboxycinnamic acid, *predominantly trans* (H_2CCN, 0.77 mg, 0.004 mmol), DMF (0.42 mL), CF_3COOH (0.015 mL) or concentrated HNO_3 (0.035 mL) or concentrated HCl (0.07 mL), in a capped vial was heated at 120 °C for 24 h. The pH values before and after reaction for CF_3COOH, conc. HNO_3, and conc. HCl are 1.74/7.16, 1.01/5.29, and 0.56/4.58, respectively. Colourless octahedral crystals were filtered, washed with MeOH and Et_2O, and dried at room temperature. Yield, 36% based on H_2CCN. Anal. Calcd for $Th_6(\mu_3\text{-}O)_4(\mu_3\text{-}OH)_4(CCN)_{12}(H_2O)_6(DMF)_{18}(H_2O)_{16}$, $C_{114}H_{210}N_{18}Th_6O_{72}$, C, 31.28; H, 4.84; N, 5.76. Found: C, 31.21; H, 4.72; N, 5.42%. IR: 1651 (s), 1593 (w), 1430 (w), 1382 (s), 1098 (w), 789 (s), 576 (m), 456 (w) cm^{-1}. Microcrystals can be obtained as followed: A mixture of $Th(NO_3)_4 \cdot 6H_2O$ (23.5 mg, 0.04 mmol), 4-carboxycinnamic acid, *predominantly trans* (3.8 mg, 0.02 mmol), DMF (0.9 mL), CF_3COOH (0.045 mL) in a capped vial was heated at 120 °C for 24 h. Colourless octahedral crystals were filtered, washed with MeOH and Et_2O, and dried at room temperature.

Th-SINAP-12. A mixture of $Th(NO_3)_4 \cdot 6H_2O$ (4.7 mg, 0.008 mmol), 1,4-phenylenediacrylic acid (H_2PEDA, 0.87 mg, 0.004 mmol), DMF (0.42 mL), HCOOH (0.05 mL)/H_2O(0.03 mL) or CF_3COOH (0.05 mL)/H_2O (0.03 mL) in a capped vial was heated at 120 °C for 24 h. The pH values before and after reaction for HCOOH and CF_3COOH are 2.10/5.68 and 1.35/6.75, respectively. Colourless octahedral crystals were filtered, washed with MeOH and Et_2O, and dried at room temperature. Yield, 36% based on H_2PEDA. Anal. Calcd for $Th_6(\mu_3\text{-}O)_4(\mu_3\text{-}OH)_4(PEDA)_6(H_2O)_6(DMF)_{16}(H_2O)_{25}$, $C_{120}H_{226}N_{16}Th_6O_{79}$, C, 31.68; H, 5.01; N, 4.93. Found: C, 31.36; H, 4.87; N, 5.22%. IR: 1651 (s), 1428 (w), 1382 (s), 981 (w), 835 (s), 696 (m), 556 (s) cm^{-1}. Microcrystals can be obtained as followed: A mixture of $Th(NO_3)_4 \cdot 6H_2O$ (23.5 mg, 0.04 mmol), 1,4-phenylenediacrylic acid (4.4 mg, 0.02 mmol), DMF (1.8 mL), concentrated HNO_3 (0.05 mL), H_2O (0.03 mL) in a capped vial was heated at 120 °C for 48 h. Colourless crystals were filtered, washed with MeOH and Et_2O, and dried at room temperature.

Th-SINAP-13. A mixture of $Th(NO_3)_4 \cdot 6H_2O$ (4.7 mg, 0.008 mmol), biphenyldicarboxylic acid (H_2BPDC, 0.97 mg, 0.004 mmol), DMF (0.38 mL), HCOOH (0.015 mL) or CF_3COOH (0.015 mL) or concentrated HNO_3 (0.03 mL) or concentrated HCl (0.06 mL) in a capped vial was heated at 120 °C for 24 h. The pH values before and after reaction for HCOOH, CF_3COOH, conc. HNO_3, and conc. HCl are 2.50/6.07, 1.64/7.42, 0.96/5.38, and 0.52/4.60, respectively. Colourless octahedral crystals were filtered, washed with MeOH and Et_2O, and dried at room temperature. Yield, 36% based on H_2BPDC. Anal. Calcd for $Th_6(\mu_3\text{-}O)_4(\mu_3\text{-}OH)_4(BPDC)_6(H_2O)_6(DMF)_{12}(H_2O)_2$, $C_{120}H_{152}N_{12}Th_6O_{52}$, C, 36.15; H, 3.85; N, 4.22. Found: C, 36.08; H, 4.06; N, 4.52%. IR: 1653 (s), 1595 (s), 1384 (vs), 1312 (w), 1091 (m), 770 (m), 576 (m), 515 (w) cm^{-1}. Microcrystalline powder can be obtained as

followed: A mixture of $Th(NO_3)_4{\cdot}6H_2O$ (23.5 mg, 0.04 mmol), biphenyldicarboxylic acid (4.8 mg, 0.02 mmol), DMF (0.79 mL), concentrated HCl (0.05 mL) in a capped vial was heated at 120 °C for 24 h. Colourless microcrystals were filtered, washed with MeOH and Et_2O, and dried at room temperature.

Th-SINAP-14. A mixture of $Th(NO_3)_4{\cdot}6H_2O$ (4.7 mg, 0.008 mmol), 4,4-azobenezenedicarboxylic acid (H_2ABDC, 1.1 mg, 0.004 mol), DMF (0.38 mL), HCOOH (0.03 mL) or concentrated HNO_3 (0.03 mL) or concentrated HCl (0.045 mL) in a capped vial was heated at 120 °C for 24 h. The pH values before and after reaction for HCOOH, conc. HNO_3, and conc. HCl are 2.25/5.16, 0.93/5.19, and 0.63/4.92, respectively. Red octahedral crystals were filtered, washed with MeOH and Et_2O, and dried at room temperature. Yield, 54% based on H_2ABDC. Anal. Calcd for $Th_6(\mu_3\text{-}O)_4(\mu_3\text{-}OH)_4(ABDC)_6(H_2O)_6(DMF)_3(H_2O)_{27}$, $C_{93}H_{139}N_{15}Th_6O_{68}$, C, 28.30; H, 3.55; N, 5.32. Found: C, 28.12; H, 3.08; N, 5.32%. IR: 1594 (s), 1556 (s), 1387 (vs), 1096 (w), 1011 (m), 875 (w), 792 (s), 706 (w), 578 (w), 533 (w) cm^{-1}.

Th-SINAP-15. A mixture of $Th(NO_3)_4{\cdot}6H_2O$ (4.7 mg, 0.008 mmol), 4,4'-stilbenedicarboxylic acid (H_2SBDC, 1.1 mg, 0.004 mmol), DMF (0.42 mL), HCOOH (0.03 mL) or CF_3COOH (0.045 mL) or concentrated HNO_3 (0.03 mL) or concentrated HCl (0.06 mL) in a capped vial was heated at 120 °C for 24 h. The pH values before and after reaction for HCOOH, CF_3COOH, conc. HNO_3, and conc. HCl are 2.13/5.37 , 1.37/6.84, 0.97/5.39, and 0.73/4.59, respectively. Colourless octahedral crystals were filtered, washed with MeOH and Et_2O, and dried at room temperature. Yield, 36% based on H_2SBDC. Anal. Calcd for $Th_6(\mu_3\text{-}O)_4(\mu_3\text{-}OH)_4(SBDC)_6(H_2O)_6(DMF)_5(H_2O)_{20}$, $C_{111}H_{151}N_5Th_6O_{63}$, C, 33.70; H, 3.85; N, 1.77. Found: C, 33.92; H, 3.39; N, 1.83%. IR: 1652 (s), 1497 (w), 1382 (w), 788 (m), 707 (w), 574 (m), 513 (w) cm^{-1}. Microcrystalline powder can be obtained as followed: A mixture of $Th(NO_3)_4{\cdot}6H_2O$ (23.5 mg, 0.04 mmol), 4,4'-stilbenedicarboxylic acid (5.4 mg, 0.02 mmol), DMF (1.8 mL), concentrated HNO_3 (0.05 mL) and H_2O (0.05 mL) in a capped vial was heated at 120 °C for 48 h. Colourless microcrystalline powder were filtered, washed with MeOH and Et_2O, and dried at room temperature.

S1.2 Characterizations

X-ray Crystallography. Single-crystal XRD data was collected on a Bruker D8-Venture single-crystal X-ray diffractometer equipped with a Turbo X-ray source (Mo Kα radiation, λ = 0.71073 Å) adopting the direct-drive rotating-anode technique and a CMOS detector. The data frames were collected using the APEX3 program and processed using the *SAINT* routine. The empirical absorption correction was applied using the SADABS program.[1] The structure was solved by Intrinsic Phasing with *ShelXT*[2] and refined with ShelXL[3] using *OLEX2*[4]. All the non-H atoms were subjected to anisotropic refinement by full-matrix program. Contributions to scattering due to these highly disordered solvent molecules were removed using the *SQUEEZE* routine of *PLATON*[5]; Structures were then refined again using the data generated. Crystal data and details of the data collection are given in Table S3.

Powder X-ray diffraction (PXRD) data were collected on were collected from 2 to 40 ° with a step of 0.02 ° on a Bruker D8 Advance diffractometer with Cu Kα

radiation (λ = 1.54178 Å). The calculated PXRD pattern was produced from the CIFs using the SHELXTL-XPOW program.

N_2 absorption and Brunauer-Emmett-Teller (BET) Analysis. The N_2 adsorption isotherms were recorded at 77 K by using a micromeritics ASAP 2020 surface area and porosity analyser. Before the adsorption measurements, the freshly prepared samples of **Th-SINAP-10/12/13**, **Th-SINAP-9**, and **Th-SINAP-11** were repeatedly exchanged with MeOH, THF, and DCM for 24 h, respectively. Then the crystals were activated with the "degas" port under the vacuum at 120 °C for 6 h. **Th-SINAP-14** was soaked in 20 mL of DCM three times over 1 h (20 min each) and subsequently immersed in 20 mL n-hexane three times over 1h (20 min each).[6] Then the crystals were activated with the "degas" port under the vacuum under room temperature.

Thermogravimetric Analysis (TGA). TGA was carried out in an N_2 atmosphere with a heating rate of 10 °C/min from 40 °C to 900 °C on a NETZSCH STA 449 F3 Jupiter instrument. TGA indicated that the solvent species were removed gradually from room temperature in all cases (Fig. S3). **Th-SINAP-13** exhibits the highest thermal stability (ca.540 °C). The initial weight loss from RT to 540 °C was 25.3%, corresponding to the loss of DMF, lattice, and coordinating water molecules (*calcd* 25.6%). **Th-SINAP-9**, **Th-SINAP-10**, **Th-SINAP-11**, **Th-SINAP-12**, **Th-SINAP-14**, and **Th-SINAP-15** are thermally stable up to *ca.*380, 470, 470, 420, 460, and 430 °C, respectively. The initial weight loss from RT to those temperatures were 34.5%, 29.3%, 38.4%, 33.3%, 24.9%, and 26.5%, respectively, which can be attributed to the removal of the guest species (*calcd* 36.2%, 30.0%, 39.1%, 38.0%, 20.6%, and 21.1%)。

X-ray photoelectron spectroscopy (XPS). The XPS data of iodine adsorbed samples were recorded on a Thermo Scientific ESCALAB 250Xi using monochromatic Al Kα (1486.8 eV) X-ray source with a spot size of 500 μm. The anode was operated at 15 kV and 10 mA.

S1.3 Adsorption Studies

Stable isotope (^{127}I) was used as a surrogate for the radioactive ones (^{129}I and ^{131}I) as their chemical properties are nearly identical.

Iodine/Cyclohexane Adsorption Measurement. Adsorption studies were performed by immersing 20 mg sample in 8 mL of a 200 mg·L^{-1} iodine/cyclohexane solution. The supernatant solution was used for each UV–vis absorbance measurement (UV-2600, SHIMADZU) periodically. After each measurement, the solution was dispensed back into the respective vial to keep the volume constant. The absorbance at maximum wavelength of iodine (λ_{max} = 522 nm) was chosen to calculate the iodine content, and the absorbance value for the original solution was normalized to 100%. The removal ratios (R) of iodine were calculated using $R = (C_0 - C_t)/C_0 \times 100\%$ (where C_0 and C_t represent the initial concentration and concentration at time t, respectively). Sorption kinetics of iodine in **Th-SINAP-10** and **Th-SINAP-12** were fitted to a pseudo-second-order kinetics model, respectively, $t/q_t = 1/h + t/q_e$ (where q_t, q_e represent the amounts of adsorbate at certain time t or at equilibrium time, h is the

initial adsorption rate, $h = kq_e^2$, and k is the rate constant) (Table S4).

The sorption isotherms of iodine in **Th-SINAP-10** and **Th-SINAP-12** were determined by adding 20 mg solid samples into 8 mL solutions with various iodine concentrations and the Langmuir and Freundlich models were used to interpret the experimental data. The linear equation of the Langmuir isotherm model is expressed as followed:

$$\frac{C_e}{q_e} = \frac{1}{q_m k_L} + \frac{C_e}{q_m}$$

Where q_m is the maximum sorption capacity corresponding to complete monolayer coverage (mg/g) and k_L is a constant indirectly related to sorption capacity and energy of sorption (L/mg), which characterizes the affinity of the adsorbate with the adsorbent. The linearized plot was obtained when we plotted C_e/q_e against C_e and q_m and k_L could be calculated from the slope and intercept.

The linear equation of Freundlich isotherm model can be expressed by:

$$\ln q_e = \ln k_F + \frac{1}{n} \ln C_e$$

Where k_F and n are the Freundlich constants related to the sorption capacity and the sorption intensity, respectively. The linear plot was obtained by plotting $\ln q_e$ against $\ln C_e$, and the values of k_F and n were calculated from the slope and intercept of the straight line. Table S5 shows the fitting results from the Langmuir and Freundlich models.

Iodine Vapour Adsorption Measurement. An open vial (20 mL) containing 50 mg samples was accurately weighted (m_0) and introduced into a glass vessel (150 mL) containing 1 g iodine. The vessel was sealed and kept in an oven at 80 °C. After certain time intervals, the vial containing the sample was weighed periodically (m_t) until the mass of it did not change. The iodine adsorption capacity can be calculated as: $wt\% = (m_t - m_0)/m_0$.

S2. FIG.S AND TABLES

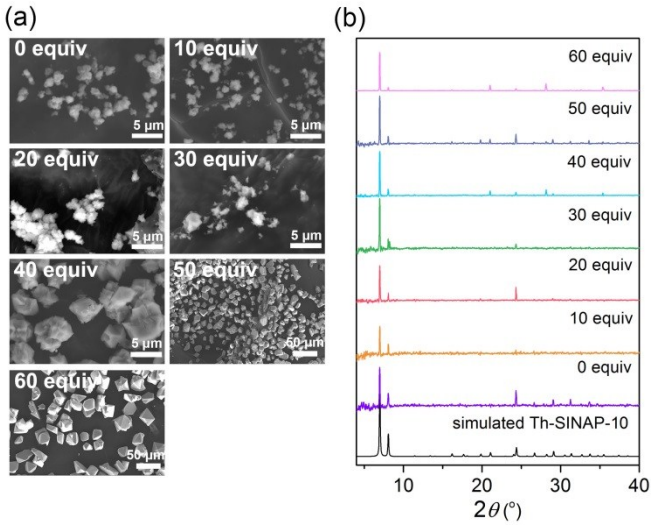

Fig. S1 SEM images and (b) PXRD patterns of **Th-SINAP-10** samples synthesized in the presence of 0, 10, 20, 30, 40, 50, and 60 equivalents of concentrated HNO_3.

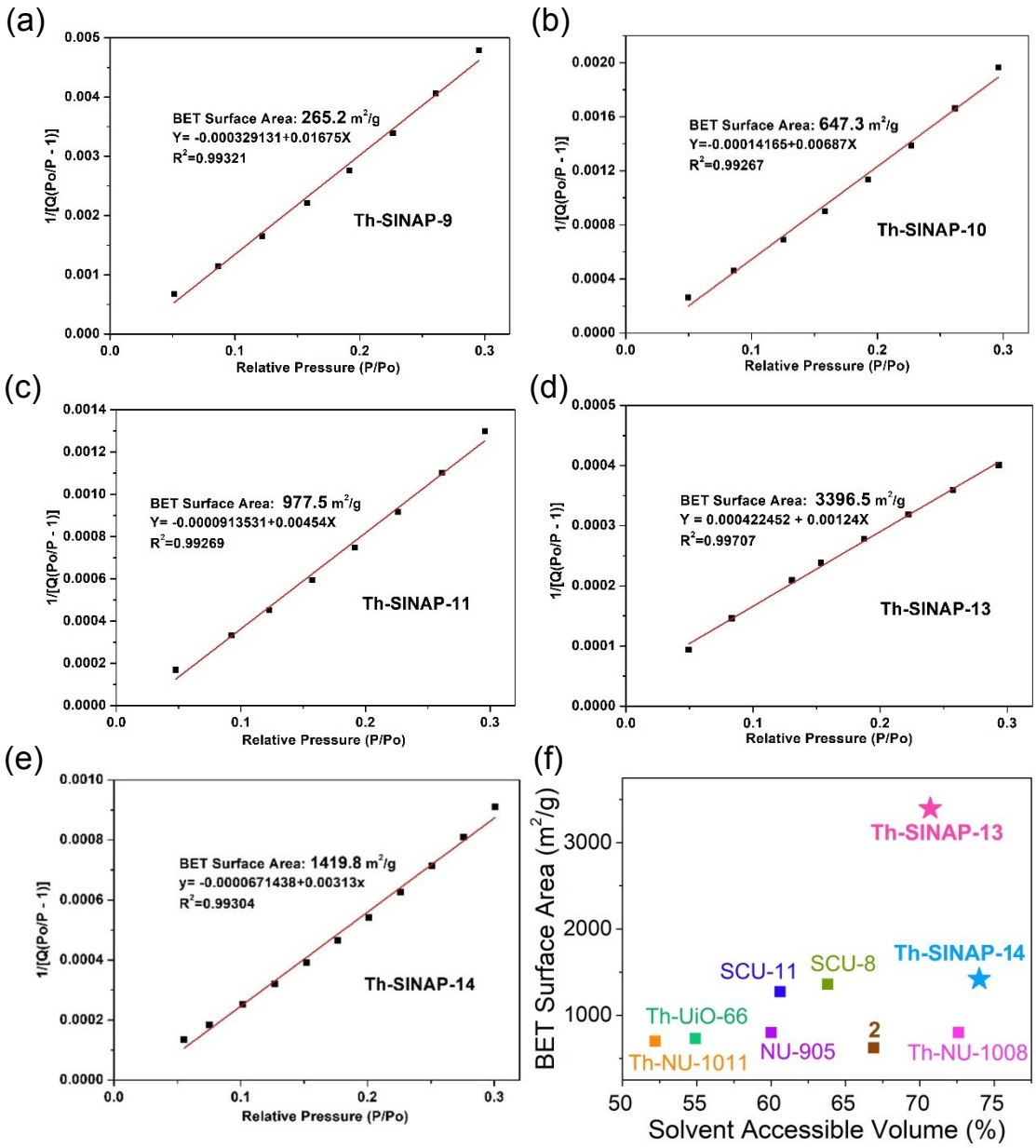

Fig. S2 BET Surface area plots of (a) **Th-SINAP-9**, (b) **Th-SINAP-10**, (c) **Th-SINAP-11**, (d) **Th-SINAP-13**, and (e) **Th-SINAP-14**. (f) Comparison of the BET surface areas and solvent accessible volumes of **Th-SINAP-13** and **Th-SINAP-14** with those of other reported thorium materials.[7-14]

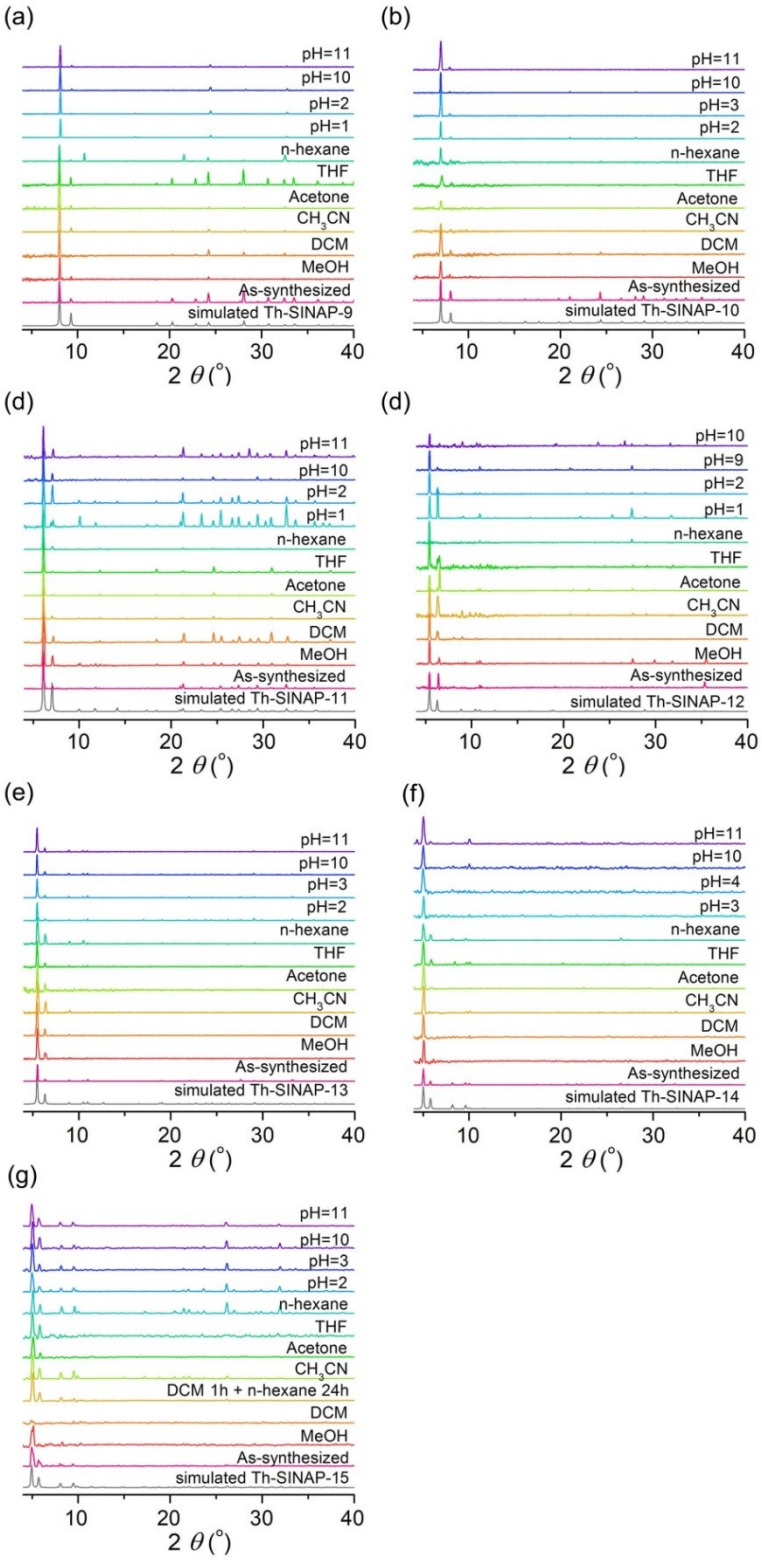

Fig. S3 PXRD patterns of (a) **Th-SINAP-9**, (b) **Th-SINAP-10**, (c) **Th-SINAP-11**, (d) **Th-SINAP-12**, (e) **Th-SINAP-13**, (f) **Th-SINAP-14**, and (g) **Th-SINAP-15** treated under various conditions. Exposing **Th-SINAP-15** to DCM for 1h resulted in the loss of its crystallinity, which however can be fully restored after soaking in hexane for 24 h.

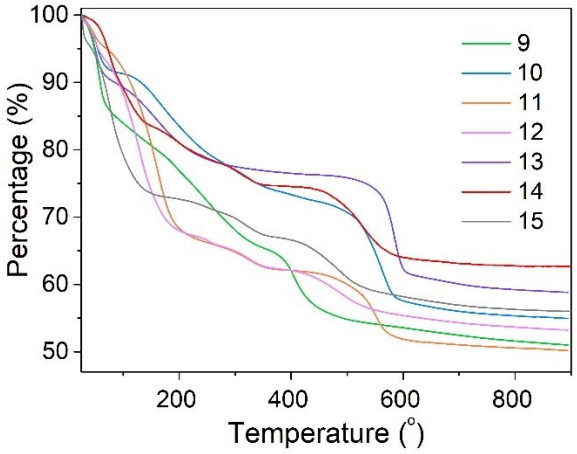

Fig. S4 The TGA plots of **Th-SINAP-n** (n = 9-15).

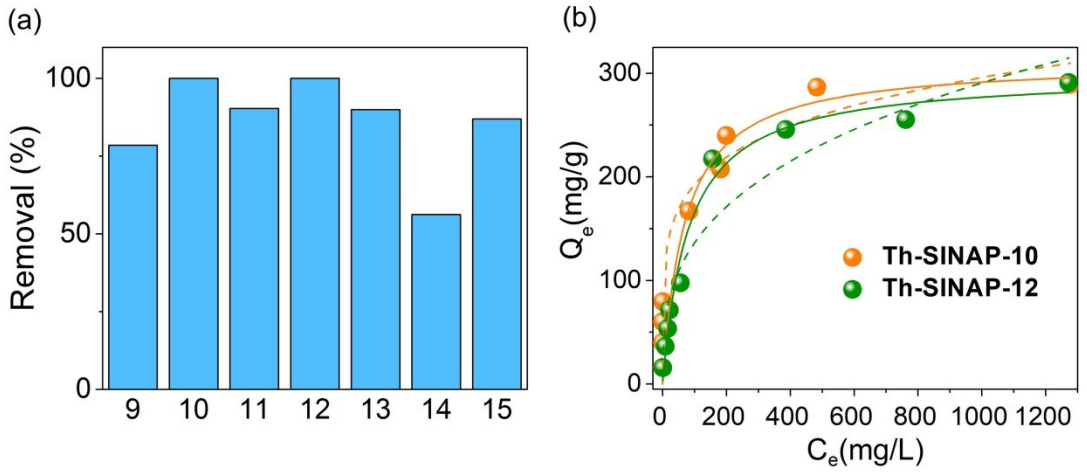

Fig. S5 (a) Removal rate of iodine from cyclohexane solutions by **Th-SINAP-n**. (b) Iodine adsorption isotherms of **Th-SINAP-10** and **Th-SINAP-12**. Solid line: Langmuir fitting; dash line: Freundlich fitting.

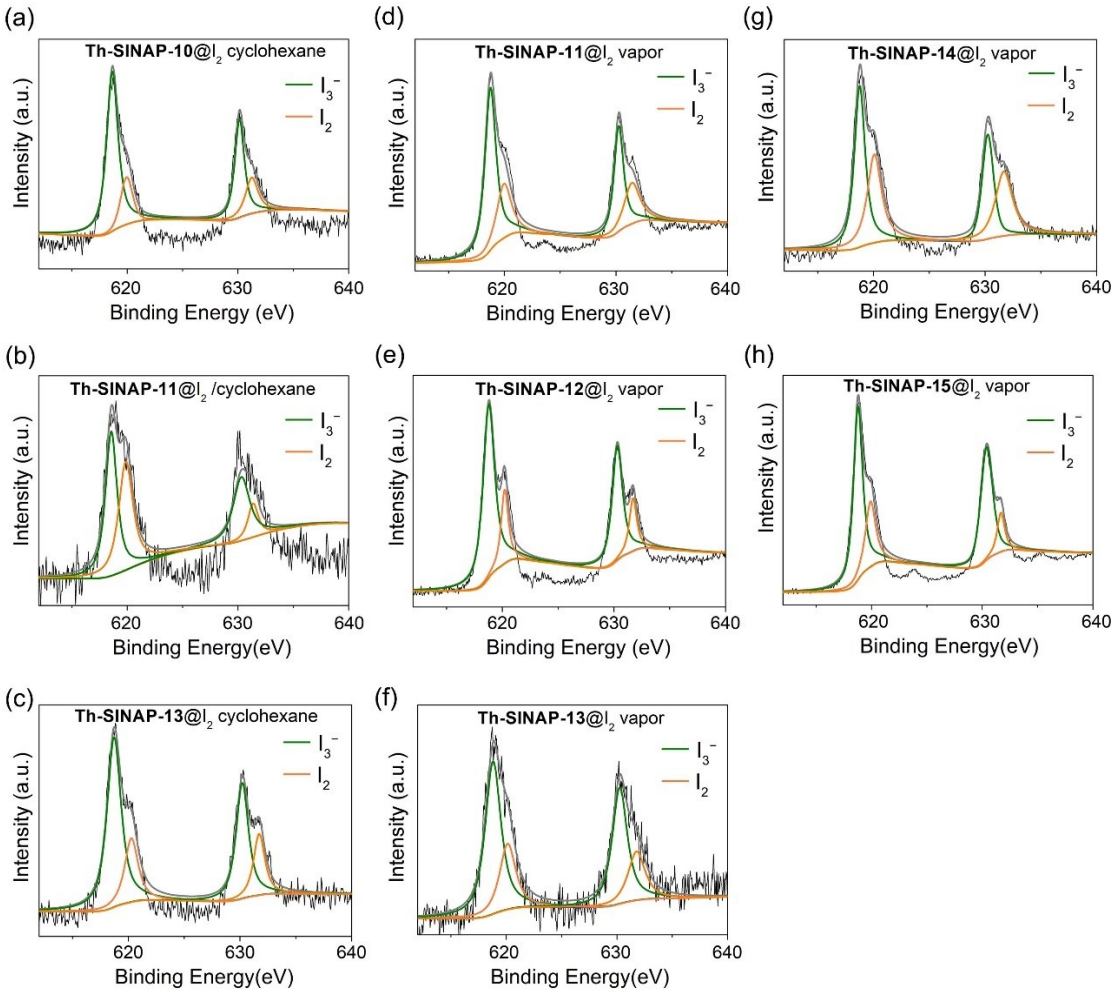

Fig. S6 XPS spectra of I_2/cyclohexane and I_2 vapour adsorbed **Th-SINAP-n**.

Table S1. Synthetic details to obtain the large single crystals of **Th-SINAP-n** (n=9-15).

Product	Metal	Ligand	Solvent	Modulator			
Code	$Th(NO_3)_4$ (mmol)	H_2L (mmol)	DMF (mL)	HCOOH (mL)	CF_3COOH (mL)	conc. HNO_3 (mL)	conc. HCl (mL)
Th-SINAP-9	0.008	0.004	0.37	0.04 pH 2.07/5.09	/	/	/
Th-SINAP-10	0.008	0.004	0.38	0.045 pH 2.12/5.04	0.03 pH 1.34/5.52	0.035 pH 0.63/5.09	/
Th-SINAP-11	0.008	0.004	0.42	/	0.015 pH 1.74/7.16	0.035 pH 1.01/5.29	0.07 pH 0.56/4.58
Th-SINAP-12	0.008	0.004	0.42	0.05 (0.03 mL H_2O) pH 2.10/5.68	/	/	/
Th-SINAP-13	0.008	0.004	0.38	0.015 pH 2.50/6.07	0.015 pH 1.64/7.42	0.03 pH 0.96/5.38	0.06 pH 0.52/4.60
Th-SINAP-14	0.008	0.004	0.38	0.03 pH 2.25/5.16	/	0.03 pH 0.93/5.19	0.045 pH 0.63/4.92
Th-SINAP-15	0.008	0.004	0.42	0.03 pH 2.13/5.37	0.045 pH 1.37/6.84	0.03 pH 0.97/5.39	0.06 pH 0.73/4.59

Table S2. Performance of HCOOH, CF_3COOH, concentrated HNO_3, and concentrated HCl as modulators for Th-MOFs synthesis.

Ligand		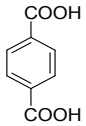	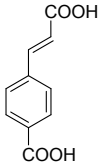	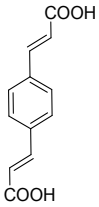	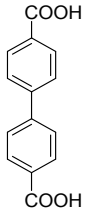	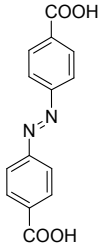	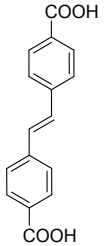
Code	**Th-SINAP-9**	**Th-SINAP-10**	**Th-SINAP-11**	**Th-SINAP-12**	**Th-SINAP-13**	**Th-SINAP-14**	**Th-SINAP-15**
HCOOH	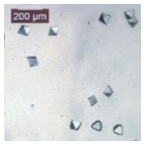	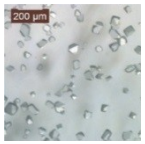		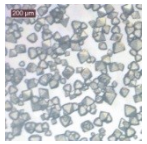	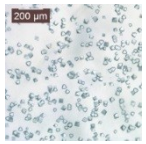	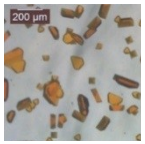	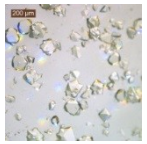
CF_3COOH		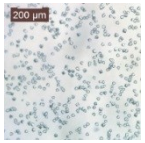	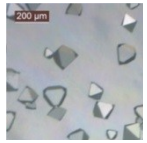	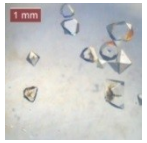			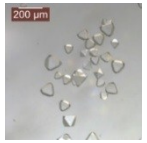
Conc. HNO_3		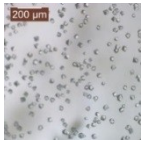	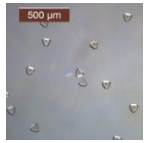		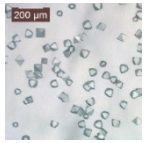	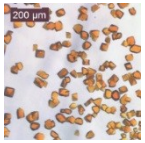	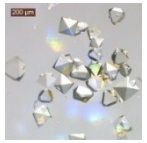
Conc. HCl					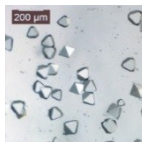	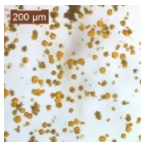	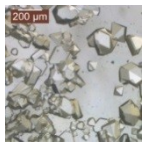

Table S3. Crystallographic Data for **Th-SINAP-n** (n=9-15).

Code	**Th-SINAP-9**	**Th-SINAP-10**	**Th-SINAP-11**	**Th-SINAP-12**	**Th-SINAP-13**	**Th-SINAP-14**	**Th-SINAP-15**
CCDC number	1981554	1981555	1981556	1981557	1981558	1981560	1981559
formula	$C_{48}H_{24}O_{78}Th_{12}$	$C_{24}H_{12}O_{19}Th_3$	$C_{60}H_{36}O_{38}Th_6$	$C_{144}H_{96}O_{76}Th_{12}$	$C_{42}H_{24}O_{19}Th_3$	$C_{84}H_{48}N_{12}O_{38}Th_6$	$C_{400}H_{250}O_{156}Th_{24}$
formula weight	4633.15	1300.46	2757.13	5826.68	1528.73	3225.58	13110.29
habit	octahedral	octahedral	octahedral	octahedral	octahedral	octahedral	octahedral
space Group	*Fm*-3*m*	*Fm*-3*m*	*Fm*-3*m*	*Fm*-3*m*	*Fm*-3*m*	*Fm*-3*m*	*Fm*-3*m*
a (Å)	19.0604(13)	21.9026(4)	25.0520(7)	28.2063(13)	27.9387(4)	30.4822(15)	30.976(4)
V (Å^3)	6924.6(8)	10507.2(6)	15722.7(13)	22440.8(18)	21808.1(9)	28323(4)	29722(10)
Z	2	8	4	2	8	4	1
T (K)	120	120	120	120	120	120	120
λ (Å)	0.71073	0.71073	0.71073	0.71073	0.71073	0.71073	0.71073
Max. 2θ (°)	54.934	59.066	54.898	41.534	68.622	54.890	50.996
ρ_{calcd} (g cm^{-3})	2.222	1.644	1.165	0.862	0.931	0.756	0.732
μ (mm^{-1})	12.913	8.520	5.697	3.994	4.113	3.170	3.021
GoF on F^2	1.097	1.066	1.051	1.140	1.057	1.109	1.234
R_1, wR_2 [I > 2σ(I)]	0.0840, 0.2042	0.0234, 0.0482	0.0651, 0.1827	0.0765, 0.2128	0.0274, 0.0600	0.0855, 0.2293	0.0573, 0.1568
R_1, wR_2 (all data)	0.1043, 0.2303	0.0338, 0.0514	0.0812, 0.2054	0.0826, 0.2203	0.0419，0.0661	0.1527, 0.3077	0.0864, 0.2038
$(\Delta\rho)_{max}$, $(\Delta\rho)_{min}$/e (Å^{-3})	6.84/ -4.17	1.02/ -1.10	2.22/ 2.10	3.73, -2.02	1.41/ -1.41	1.87/ -2.30	2.02/ -1.06

Table S4. Iodine adsorption capacities of selected MOFs.

Materials	Iodine uptake (wt%)	Iodine uptake (I_2 per metal atom)	Ref.
$Zr_6O_4(OH)_4(sdc)_6$	279 [a]	**1.98**	15
Th-TTHA	53 [b]	**0.96**	16
ZIF-8	125 [c]	**1.75**	17
HKUST-1	175 [c]	**1.08**	18
Th-SINAP-8	47 [c]	**1.22**	19
MOF-808	218 [c]	**1.94**	20
NU-1000	145 [c]	**2.40**	20

Test conditions: [a] Iodine vapor adsorption, room temperature. [b] Iodine adsorption from cyclohexane solution, room temperature. [c] Iodine vapor adsorption, 75–80 ^oC.

Table S5. Kinetic parameters of the pseudo-second-order model for iodine adsorption toward **Th-SINAP-10** and **Th-SINAP-12**.

	c_0 (mg·kg^{-1})	M/V (mg·g^{-1})	q_0 (mg·g^{-1})	Removal (%)	Second-order kinetic model			
					q_e (mg·g^{-1})	h (mg·g^{-1}·h^{-1})	k (g·mg^{-1}·h^{-1})	R^2
Th-SINAP-10	200	2.5	80	99.83	76.3	228.79	0.0393	0.970
Th-SINAP-12	200	2.5	80	97.32	82.93	47.45	0.0069	0.997

Table S6. Fitting results of the sorption isotherms according to the Langmuir and Freundlich equations

Sample	Langmuir			Freundlich		
	Q_m (mg/g)	K_L (L/mg)	R^2	k_F (L^n/mol^{n-1}g)	n	R^2
Th-SINAP-10	292.4	0.04288	0.99438	76.18694	5.05076	0.96204
Th-SINAP-12	298.5	0.01391	0.99273	16.80422	2.32035	0.96185

S3. REFERENCES

1. G. M. Sheldrick, 1996.
2. G. M. Sheldrick, *Acta Crystallogr. Sect. A: Found. Adv.*, 2015, **71**, 3.
3. G. M. Sheldrick, *Acta Crystallogr. Sect. C: Struct. Chem.*, 2015, **71**, 3.
4. O. V. Dolomanov, L. J. Bourhis, R. J. Gildea, J. A. K. Howard and H. Puschmann, *J. Appl. Cryst.*, 2009, **42**, 339.
5. A. L. Spek, *Acta Crystallogr. Sect. C: Struct. Chem.*, 2015, **71**, 9.
6. J. Ma, A. P. Kalenak, A. G. Wong-Foy and A. J. Matzger, *Angew. Chem. Int. Ed.*, 2017, **56**, 14618.
7. Y. Li, Z. Yang, Y. Wang, Z. Bai, T. Zheng, X. Dai, S. Liu, D. Gui, W. Liu, M. Chen, L. Chen, J. Diwu, L. Zhu, R. Zhou, Z. Chai, T. E. Albrecht-Schmitt and S. Wang, *Nat. Commun.*, 2017, **8**, 1354.
8. Y. Wang, W. Liu, Z. Bai, T. Zheng, M. A. Silver, Y. Li, Y. Wang, X. Wang, J. Diwu, Z. Chai and S. Wang, *Angew. Chem. Int. Ed.*, 2018, **57**, 5783.
9. E. A. Dolgopolova, O. A. Ejegbavwo, C. R. Martin, M. D. Smith, W. Setyawan, S. G. Karakalos, C. H. Henager, H.-C. zur Loye and N. B. Shustova, *J. Am. Chem. Soc.*, 2017, **139**, 16852.
10. P. Li, X. Wang, K.-i. Otake, J. Lyu, S. L. Hanna, T. Islamoglu and O. K. Farha, *ACS Appl. Nano Mater.*, 2019, **2**, 2260.
11. P. Li, S. Goswami, K.-i. Otake, X. Wang, Z. Chen, S. L. Hanna and O. K. Farha, *Inorg. Chem.*, 2019, **58**, 3586.
12. C. Falaise, J.-S. Charles, C. Volkringer and T. Loiseau, *Inorg. Chem.*, 2015, **54**, 2235.
13. Y. Li, Z. Weng, Y. Wang, L. Chen, D. Sheng, Y. Liu, J. Diwu, Z. Chai, T. E. Albrecht-Schmitt and S. Wang, *Dalton Trans.*, 2015, **44**, 20867.
14. P. Li, N. A. Vermeulen, C. D. Malliakas, D. A. Gómez-Gualdrón, A. J. Howarth, B. L. Mehdi, A. Dohnalkova, N. D. Browning, M. O'Keeffe and O. K. Farha, *Science*, 2017, **356**, 624.
15. R. J. Marshall, S. L. Griffin, C. Wilson and R. S. Forgan, *Chem. Eur. J.*, 2016, **22**, 4870.
16. N. Zhang, L.-X. Sun, F.-Y. Bai and Y.-H. Xing, *Inorg. Chem.*, 2020, **59**, 3964.
17. D. F. Sava, M. A. Rodriguez, K. W. Chapman, P. J. Chupas, J. A. Greathouse, P. S. Crozier and T. M. Nenoff, *J. Am. Chem. Soc.*, 2011, **133**, 12398.
18. D. F. Sava, K. W. Chapman, M. A. Rodriguez, J. A. Greathouse, P. S. Crozier, H. Zhao, P. J. Chupas and T. M. Nenoff, *Chem. Mater.*, 2013, **25**, 2591.
19. Z.-J. Li, Z. Yue, Y. Ju, X. Wu, Y. Ren, S. Wang, Y. Li, Z.-H. Zhang, X. Guo, J. Lin and J.-Q. Wang, *Inorg. Chem.*, 2020, **59**, 4435.
20. P. Chen, X. He, M. Pang, X. Dong, S. Zhao and W. Zhang, *ACS Appl. Mater. Interfaces*, 2020, **12**, 20429.